



Cite this: *Green Chem.*, 2025, **27**, 1895

## Recent advances in the preparation, properties, and applications of lignin-based hydrogels and adhesives

Linmeng Huo,<sup>a,b</sup> Yumiao Lu,<sup>\*,a,b</sup> Wei-Lu Ding,<sup>a,b</sup> Yanlei Wang,<sup>a,b</sup> Xuehui Li  <sup>d</sup> and Hongyan He  <sup>\*,a,b,c</sup>

Lignin, as a renewable and environmentally friendly resource, serves as the primary source of aromatic compounds in nature. Harnessing lignin for high-value applications is essential for addressing energy and environmental challenges, and thus it is crucial to develop high-performance lignin-based materials through advanced materials technologies. Among various lignin-based materials, hydrogels and adhesives have garnered significant attention due to their simple preparation methods and excellent properties. This review summarizes recent advancements in the preparation strategies, structural features, functional attributes, and applications of lignin-based hydrogels and adhesives. First, the structural characteristics and utilization methods of lignin are analyzed based on its source. Then, the preparation methods of lignin-based hydrogels are detailed, offering an in-depth comparison of the advantages and disadvantages of physical and chemical crosslinking methods. The functional attributes of lignin-based hydrogels and their applications in fields such as flexible sensing and energy storage are thoroughly reviewed. Additionally, this review discusses the preparation methods of lignin-based adhesives and their ongoing development for wood bonding applications. Finally, future directions for the development of lignin-based hydrogels and adhesives are explored. This review provides fundamental knowledge on the preparation, application, and development of lignin-based hydrogels and adhesives, offering valuable insights for the efficient conversion and utilization of lignin.

Received 31st October 2024,  
Accepted 6th January 2025  
DOI: 10.1039/d4gc05491a  
[rsc.li/greenchem](http://rsc.li/greenchem)

### Green foundation

1. Advances in green chemistry have been discussed in the context of lignin-based materials, focusing on innovative synthesis methods and potential high-value applications of lignin-based hydrogels and adhesives that are eco-friendly.
2. The study of lignin-based hydrogels and adhesives is of significant wider interest due to their potential to replace non-renewable and less sustainable materials, offering a green alternative in different fields, including flexible sensing, energy storage, biomedical and adsorption applications.
3. The future of this field is poised for growth with the development of more sustainable and efficient lignin-based materials. The insights from this review will aid in shaping green chemistry science by providing a comprehensive understanding of lignin's preparation, application, and development, guiding future research towards environmentally friendly and high-performance materials.

## 1. Introduction

The over-reliance on and extensive consumption of fossil energy has led to increasing environmental issues. Given the non-renewable nature of fossil energy, the search for sustainable and eco-friendly alternatives has become imperative.<sup>1–3</sup> Among the various renewable energy sources, biomass stands out for its availability, abundance, and renewability.<sup>4–7</sup> In recent years, interest and investment in biomass technologies have increased, with a strong focus on promoting industrial

<sup>a</sup>CAS Key Laboratory of Green Process and Engineering, State Key Laboratory of Mesoscience and Engineering, Beijing Key Laboratory of Ionic Liquids Clean Process, Institute of Process Engineering, Chinese Academy of Sciences, Beijing 100190, China. E-mail: [ymlv@ipe.ac.cn](mailto:ymlv@ipe.ac.cn), [hyhe@ipe.ac.cn](mailto:hyhe@ipe.ac.cn)

<sup>b</sup>University of Chinese Academy of Sciences, Beijing 100049, China  
<sup>c</sup>Longzihu New Energy Laboratory, Zhengzhou Institute of Emerging Industrial Technology, Zhengzhou 450000, China

<sup>d</sup>School of Chemistry and Chemical Engineering, State Key Laboratory of Pulp & Paper Engineering, South China University of Technology, Guangzhou, 510640, China

development. Biomass encompasses many materials, including plants, animals, and microorganisms. Among these, lignocellulose, which is abundant in wood and agricultural byproducts like straw, bran, and bagasse, shows great promise as a resource.<sup>8–11</sup> Lignocellulose is mainly composed of cellulose (35–50%), hemicellulose (20–30%), and lignin (20–30%).<sup>12–15</sup> Cellulose is a highly crystalline linear polysaccharide with glucose units linked by glycosidic bonds.<sup>16</sup> At the same time, hemicellulose is an amorphous polysaccharide comprising structural units like xylose, arabinose, and galactose.<sup>8</sup> Lignin, an aromatic polymer, is primarily constructed from phenylpropane units connected by ether and carbon–carbon bonds.<sup>17,18</sup> While cellulose and hemicellulose have been successfully commercialized, the efficient conversion and utilization of lignin continue to pose significant challenges.

Lignin's structure is rich with various functional groups, including aromatic rings and phenolic and alcoholic hydroxyl, carbonyl, methoxy, and carboxyl groups. These diverse chemical groups make lignin a valuable resource for producing high-value products through various chemical reactions.<sup>19–21</sup> However, its complex structure makes the industrial utilization ratio extremely low, at a mere 2%, with most of it being burned as waste, causing severe environmental pollution and resource wastage.<sup>22–24</sup> Converting lignin into high-value-added products is crucial for fully exploiting biomass resources.<sup>25</sup> In recent years, extensive attention has been devoted to lignin conversion and utilization, leading to the emergence of a variety of lignin-based functional materials, such as modified phenolic resins,<sup>26</sup> carbon fibers,<sup>27</sup> water reducers,<sup>28</sup> adsorbents,<sup>29</sup> surfactants,<sup>30</sup> hydrogels,<sup>31</sup> and adhesives.<sup>32</sup> Among these, lignin-based hydrogels and adhesives have emerged as critical research areas due to their simple preparation methods and exceptional functional features, which are experiencing rapid development.

This review highlights the recent advancements in lignin-based hydrogels and adhesives. It begins by introducing lignin's different types and structural features, followed by an analysis of their respective uses in hydrogels and adhesives. The preparation methods of lignin-based hydrogels are then explored and compared. Finally, the functional performance and application fields of these two materials are discussed, focusing on their opportunities and challenges in development.

## 2. Structure of lignin

Lignin mainly contains three elements, C, H, and O. It is a complex polymer composed of three main structural units, *viz.* *p*-hydroxyphenyl units, guaiacyl units, and syringyl units, which are connected by various interunit C–O and C–C linkages.<sup>33,34</sup> The conversion and utilization of lignin mainly include two ways: one is lignin depolymerization by selectively cracking C–C/C–O bonds to obtain lignin monomers and oligomers, which can be further converted into high-value-added chemicals and fuels.<sup>35–37</sup> The other is the direct use of unpoly-

merized lignin to prepare materials and products with different functions based on the functional groups in its structure (Fig. 1). However, lignin often faces challenges such as limited solubility and low reactivity. Chemical modification is usually employed to enhance its utility and performance in various applications. This can be achieved through various techniques, including sulfonation, amination, graft copolymerization, esterification, and oxidation. Each of these methods targets specific improvements: enhancing water solubility,<sup>38</sup> boosting reactivity and compatibility,<sup>39</sup> and bolstering thermal stability.<sup>40,41</sup>

Generally, lignin can be categorized into natural lignin and industrial lignin based on its source (Fig. 2a).<sup>42</sup> Natural lignin refers to unmodified lignin in its original state<sup>43</sup> and is commonly used for analyzing the structural characteristics of lignin. In contrast, industrial lignin is derived from lignocellulose or recovered from industrial wastes and by-products. Its separation typically involves complex solvent-based treatment processes, including acid treatment and pulp and paper extraction processes, which can significantly change the lignin structure. For example, dissolution and depolymerization are inevitably accompanied by the condensation of lignin, leading to the formation of additional C–C bonds, which complicates the subsequent transformation and utilization.<sup>44,45</sup> Despite these challenges, industrial lignin is produced in vast quantities, with the paper industry alone generating 50–60 million tons annually.<sup>46</sup> Therefore, due to its abundance, industrial lignin is mainly utilized in practical applications.

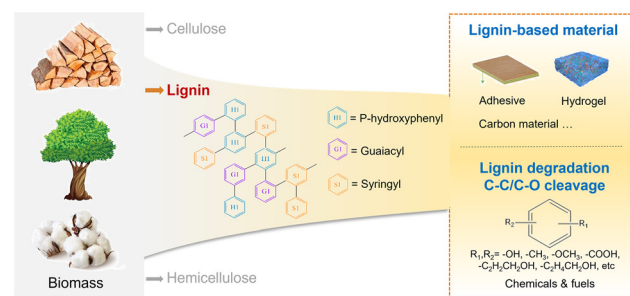


Fig. 1 Conversion and utilization of lignin.

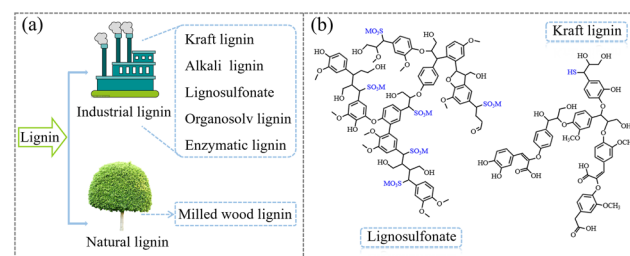


Fig. 2 (a) Different types of lignin. (b) The structure of lignosulfonate and kraft lignin.<sup>47,48</sup> [Reproduced from ref. 47 and 48 with permission from Wiley, copyright of 2022.]

## 2.1 Industrial lignin

Industrial lignin retains its inherent macromolecular skeleton and basic functional groups while undergoing chemical modification that introduces various functional groups and alters its molecular architecture. Typically, industrial lignin comes from the pulp and paper industry and bio-refining process. Depending on the separation techniques employed, it can be classified into several types: kraft lignin, lignosulfonate, alkali lignin, organosolv lignin, and enzymatic lignin.<sup>49–51</sup> Kraft lignin, a by-product of kraft pulping, is characterized by a highly concentrated and cross-linked network structure.<sup>52,53</sup> The pulping process breaks aryl ether bonds, resulting in a large number of phenolic hydroxyl groups, while the sulfur-containing compounds used in this process lead to a sulfur group content of 1–3%,<sup>54</sup> as shown in Fig. 2b. Lignosulfonate, another by-product, is derived from sulfite pulping waste liquid,<sup>54,55</sup> and refers to a diverse class of substances including sodium, calcium, magnesium and ammonium lignosulfonates.<sup>56</sup> During sulfite pulping, metal sulfites react with lignin, incorporating sulfonic acid groups into the aliphatic side chains, resulting in a sulfur content between 3.5% and 8.0%.<sup>52</sup> Alkaline lignin is obtained from alkaline pulping,<sup>50</sup> and unlike kraft lignin and lignosulfonate, it does not contain sulfur. Its structure is closer to that of natural lignin, making it more conducive to chemical modifications.<sup>57</sup> Organosolv lignin is produced by treating wood or plant raw materials with a suitable organic solvent under specific conditions, involving steps like dissolution, filtration, washing, precipitation, and drying.<sup>58</sup> Due to its relatively simple separation process, only a small number of phenolic hydroxyl groups undergo condensation, and its structure remains closer to that of natural lignin. Enzymatically hydrolyzed lignin comes from the cellulosic ethanol refining process, where cellulolytic enzymes are used to break down cellulose. However, this lignin often contains impurities such as carbohydrate and protein residues in the structure.<sup>45</sup>

## 2.2 Natural lignin

During the extraction process, natural lignin exhibits strong reactivity, making it prone to autopolymerization and oxidation reactions, which cause significant structural changes. As a result, the extraction of natural lignin remains a challenge.<sup>45,49,59</sup> Currently, milled wood lignin (MWL) is recognized for having the most structural resemblance to natural lignin.<sup>60</sup> The method for obtaining MWL was pioneered by Beckman in 1954, which involves grinding wood powder in a non-swelling solvent at room temperature, followed by dioxane solvent extraction to isolate the lignin.<sup>61</sup> However, this intensive milling process can induce structural changes in the lignin, particularly an increase in phenolic groups due to the breaking of the  $\beta$ -aryl ether bond during ball milling. Several methods have since been developed to extract natural lignin.<sup>42</sup> Under mild conditions, without the use of acidic or alkaline catalysts, lignin with minimal structural changes can be separated using organic solvent extraction. However, the extraction

rate remains low, typically under 10%. To increase lignin yield, additional acid is often applied during the extraction process. For example, at 145 °C, a mixture of 80 wt%  $\gamma$ -valerolactone and 20 wt% water, with a small amount of sulfuric acid, can be used to extract lignin from corn stover with a yield exceeding 70%.<sup>62</sup> Acidic deep eutectic solvents (DESs) or neutral DESs with added acid are also used to fractionate lignin while preserving its natural structure. Lignin obtained from switchgrass reaches a yield of over 50% using choline chloride/ethylene glycol (1 : 2) and 1.0%  $H_2SO_4$ , with a structure closely resembling that of MWL.<sup>63</sup> Additionally, ionic liquids with mild acidity can be used for lignin separation. For instance, lignin extracted from poplar using 1-ethyl-3-methylimidazole acetate retains a structure similar to that of MWL, apart from differences in molecular weight and the ratio of sinapyl alcohol to coniferyl alcohol.<sup>64</sup>

## 3. Lignin-based hydrogels

Hydrogels are a class of hydrophilic polymers characterized by their three-dimensional network structure. They are valued for their excellent biocompatibility and superior water retention abilities, making them widely applicable in fields such as biomedicine and flexible sensing (Fig. 3a). In recent years, the development of environmentally friendly, bio-based polymer hydrogels has garnered increasing attention. These hydrogels are primarily composed of natural biological materials, such as lignin, chitosan, collagen, hyaluronic acid, *etc.* Each type of hydrogel possesses distinct properties and holds application prospects across various gel-related fields. For example, chitosan-based hydrogels are renowned for their excellent biocompatibility and hydrophilicity, making them ideal for wound dressings and drug carriers.<sup>65</sup> Meanwhile, collagen-based and hyaluronic acid-based hydrogels, with their high biological activity, find wide applications in the medical field, particularly in tissue engineering.<sup>66</sup> Compared with these hydrogels, lignin-based hydrogels have shown great potential for hydrogel synthesis due to their low cost, favorable biocompatibility, and inherent biological activities such as anti-oxidant and antibacterial properties. Lignin-based hydrogels exhibit diverse properties depending on the structure of lignin and the synthesis methods, making them suitable for a wide range of applications.<sup>41</sup>

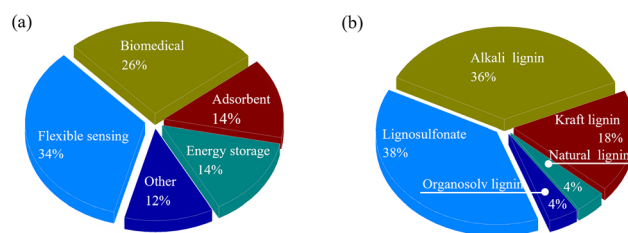


Fig. 3 Distribution of (a) applications and (b) types of lignin-based hydrogels from 50 references published from 2018 to 2024.<sup>23,28,29,31,67–112</sup>

### 3.1 Synthesis methods of lignin-based hydrogels

Both natural and industrial lignins serve as viable precursors for preparing hydrogels. Natural lignin, akin to its counterparts in plants, boasts commendable biocompatibility and biodegradability. However, to synthesize lignin-based hydrogels, natural lignin generally needs to be purified, modified, or blended with other polymers. Industrial lignin, on the other hand, has already undergone separation, extraction and chemical modification. Consequently, hydrogels synthesized from industrial lignin typically exhibit enhanced mechanical properties and chemical stability. Fig. 3b illustrates the distribution and proportion of different lignin types used in the synthesis of lignin-based hydrogels. It is clear that industrial lignin is utilized far more frequently than natural lignin in these applications. Among the various types of industrial lignin, lignosulfonate stands out as the most prevalent form for hydrogel production.

Generally, lignin-based hydrogels are typically formed through the chemical and/or physical crosslinking of monomers and/or polymers. Hydrogels prepared *via* physical crosslinking rely on non-covalent bonds to maintain their structure. These bonds confer a weaker network force but create a reversible structure, offering benefits such as reusability and environmental friendliness. On the other hand, chemically crosslinked hydrogels rely on covalent bonds, providing a more stable and permanent structure. However, this method often requires initiators and crosslinking agents, some of which may possess toxic properties.<sup>113</sup>

Physical crosslinking encompasses various interactions, including hydrogen bonding, electrostatic and hydrophilic/hydrophobic interactions, crystallization, host-guest interaction, and chain entanglement. Hydrogen bonding, a weak electrostatic interaction between hydrogen atoms and electro-negative atoms like O, N, or F, plays a crucial role in the construction of hydrogels with high strength and excellent self-healing capabilities. For instance, incorporating 2.5 wt% lignin (without further purification) into a polyurethane (HPU) hydrogel results in a twofold increase in Young's modulus and a threefold increase in tensile strength due to the formation of hydrogen bonds.<sup>107</sup> By further increasing the mass fraction of lignin to 3%, the mechanical properties can be further increased. For example, the hydrogel composed of lignin (molecular weight  $M_w = 4300$ ), hydroxyethyl cellulose (HEC) and PVA, which forms multiple hydrogen bonds, exhibits a sevenfold increase in the maximum storage modulus and a twentyfold increase in elongation, respectively.<sup>69</sup> Additionally, the dynamic hydrogen bonding and the reversible complexation of diol borax endow the hydrogel with self-healing properties.

Hydrogels often exhibit a range of properties due to the synergistic effects of multiple physical crosslinking mechanisms. For example, a new hydrogel formed by blending 7 wt% lignosulfonate (without further purification) with polyethyl-pirodanone leverages both hydrophobic interactions and hydrogen bonding. This hydrogel, when cut in half, can self-

fuse within 15 minutes without an external force, achieving an adhesion strength of 66.6 kPa to wood, and demonstrating strong self-healing and adhesive properties.<sup>89</sup> As shown in Fig. 4a, an amphoteric hydrogel (SML/QCS/PVA) electrolyte was constructed by using lignin modified with sulfomethyl functional groups (SML) and quaternized chitosan (QCS). The network structure of SML/QCS/PVA is supported by hydrogen bonds formed between hydroxyl, amino, and sulfonic acid groups, as well as electrostatic interactions between quaternary amine groups and sulfonic acid groups. This hydrogel exhibits high ionic conductivity (46.64 mS cm<sup>-1</sup>), an impressive tensile strain of 927.32%, and a compressive strain of 85% under ambient conditions.<sup>109</sup> In Fig. 4b, a hydrogel is constructed by mixing chitosan and PVA with sodium lignin sulfonate with a molecular weight of 534.51, in which the mass fraction of lignin is 4%. The cationic amino and sulfonic groups in chitosan form ionic bonds and engage in hydrogen bonding with the hydroxyl groups of PVA. Meanwhile, PVA contributes to the formation of a three-dimensional cross-linked network through extensive hydrogen bonding and molecular crystallization along its chains, creating multiple cross-linking points.<sup>87</sup> The hydrogel achieves a tensile strength of 108.58 kPa and an elongation at break of 200.8%, showcasing its remarkable mechanical performance. Chain entanglements, which involve the intertwining and interlocking of polymer chains, play a crucial role in constructing lignin-based hydrogels with enhanced mechanical properties and flexibility. For example,

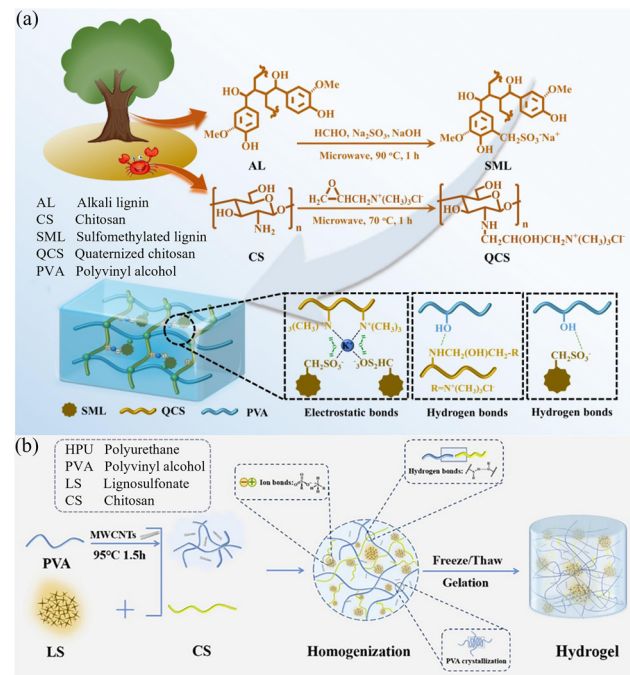


Fig. 4 Different interactions in lignin-based hydrogels prepared by the physical crosslinking method.<sup>87,109</sup> (a) Electrostatic bonds and hydrogen bonds. [Reproduced from ref. 109 with permission from Elsevier, copyright of 2024.] (b) Ionic bonds and hydrogen bonds. [Reproduced from ref. 87 with permission from American Chemical Society, copyright of 2023.]

in hydrogels where dense entanglements greatly outnumber crosslinks, there is a significant increase in toughness, comparable to that of double-network hydrogels, along with a notable enhancement in fatigue resistance.<sup>114</sup> In the case of all-wood hydrogels, the presence of a large number of hydroxyl groups in lignin, cellulose, and PVA chains promotes the formation of entanglements. These entanglements, in conjunction with hydrogen bonding and van der Waals forces, contribute to a highly cross-linked network, which endows the hydrogel with a high tensile strength and good flexibility in the longitudinal direction.<sup>77</sup>

In contrast to physical crosslinking, chemically crosslinked hydrogels are formed through covalent bonds, which provide enhanced mechanical strength and stability. The mechanical properties of hydrogels are crucial for their specific applications. In tissue engineering, they must possess sufficient strength to support cell growth and regeneration. For drug delivery, stability is essential for a controlled release. In soft robotics and wearable devices, the appropriate balance of elasticity and resilience is required. The most common method of chemical crosslinking is radical polymerization. For example, as depicted in Fig. 5a, a hydrogel can be synthesized by combining lignin, isolated from wheat straw ( $M_w = 2820$ ), with montmorillonite (MMT), using *N,N'*-methylene-bis-acrylamide (NMBA) as the crosslinking agent and MMT as the inorganic filler. The redox initiator system abstracts hydrogen atoms from the hydroxyl groups of lignin, creating free radicals that

act as active sites. Subsequently, poly(acrylic acid) (PAAc) is grafted onto the lignin. After grafting, PAA, NMBA, and montmorillonite interconnect to form the hydrogel.<sup>110</sup> An all-lignin hydrogel can also be synthesized through a chemical crosslinking reaction between kraft lignin and polyethylene glycol diglycidyl ether, exhibiting good pH-responsive behavior.<sup>81</sup> Moreover, the mechanical properties of lignin-based hydrogels can be further enhanced by crosslinking chemically modified lignin with other monomers. For instance, compression properties are improved by initiating with ammonium persulfate and polymerizing with chloroacetic acid-modified xylan and tetramethylenediamine.<sup>73</sup> The storage modulus of a hydrogel, obtained by radical polymerization of organosolv lignin ( $M_w = 3109$ ) modified with 2-hydroxyethyl methacrylate groups, increases by three orders of magnitude.<sup>103</sup> The introduction of metal ions can further improve the conductivity of lignin-based hydrogels. Hydrogels prepared with a lignosulfonate-Al<sup>3+</sup> composite system demonstrate excellent electrical output stability. In this system, the semi-quinone radicals generated by lignin oxidation with ammonium persulfate initiate the polymerization of an acrylic monomer into polyacrylic acid polymer chains. Al<sup>3+</sup> ions then crosslink these polymer chains into an ionic hydrogel at room temperature through electrostatic interactions, contributing to the hydrogel's stability and functionality.

Beyond free radical crosslinking, various other crosslinking techniques are employed. One such method is graft copolymerization,<sup>68,110,115</sup> as exemplified by the grafting of 3-allyl glycidyl ether onto lignin to synthesize 3-allyl oxygen-2-hydroxypropyl lignin (AHP-lignin) through an etherification reaction. AHP-lignin, a pivotal component in hydrogel formation, then participates in a polymerization reaction with acrylic acid (AA), facilitated by the crosslinking agent *N,N'*-methylenebisacrylamide. In this process, AHP-lignin not only engages in the polymerization with AA but also serves as a crosslinking agent, bridging AA molecules and thereby constructing the network structure of AHP-lignin/PAA hydrogel.<sup>115</sup>

Additionally, an emerging area of research focuses on synthesizing hydrogels through a hybrid approach that combines physical and chemical cross-linking. This composite technique merges the rapid response of physical cross-linking with the enduring stability offered by chemical cross-linking, thereby equipping the hydrogel with a more versatile array of properties. For example, Fig. 5b illustrates the network of AHP-lignin/PAA hydrogels, which are constructed by the chemical and physical crosslinking between AA and AHP-lignin. These hydrogels exhibit several desirable features, including UV shielding, antioxidant properties, electrical conductivity, strong adhesion, and enhanced mechanical strength.

In addition to mechanical properties, other properties such as biodegradability and water absorption capacity are equally important. Biodegradability is crucial in biomedical and environmental applications. For example, in drug delivery, the hydrogel should degrade harmlessly once the medication has been released.<sup>116</sup> In environmental applications, biodegradable hydrogels can reduce waste and pollution.<sup>110</sup> Water

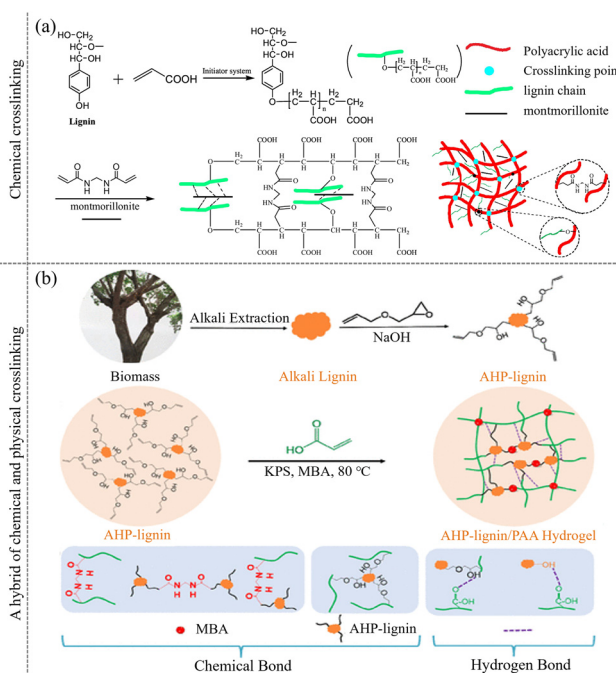


**Fig. 5** Chemical and physical crosslinking of lignin-based hydrogels.<sup>110,115</sup> (a) The preparation diagram of a composite hydrogel by combining lignin and montmorillonite. [Reproduced from ref. 110 with permission from Elsevier, copyright of 2019.] (b) Preparation of AHP-lignin/PAA hydrogel. [Reproduced from ref. 115 with permission from American Chemical Society, copyright of 2022.]

absorption capacity is vital for applications where the hydrogel is expected to maintain a moist environment or absorb excess fluids. In the case of wound dressings, a high water absorption capacity is beneficial for keeping the wound bed clean and facilitating the healing process.<sup>86</sup> Furthermore, other properties such as biocompatibility and chemical stability are also important depending on the specific application.<sup>75</sup>

### 3.2 Application of lignin-based hydrogels

**3.2.1 Flexible sensing.** Lignin-based hydrogels have attracted extensive attention in the field of flexible sensing due to their exceptional biocompatibility and biodegradability. These hydrogels, when integrated into wearable devices, establish effective contact and adhesion with human skin, showcasing good recoverability even after repeated deformation. They can monitor various static and dynamic signals in real time, such as human movement, heartbeat, pulse, and blood pressure. The hydrogel prepared by simply mixing lignosulfonate in solution exhibits excellent adhesion to different materials, including stainless steel, plexiglass, and paper. This superior adhesion is attributed to the numerous hydrogen bonds formed between the hydrogel's hydroxyl, sulfonic acid, and carboxyl groups and the corresponding groups on these materials.<sup>100</sup>

Moreover, the adhesive properties of lignin-based hydrogels can be further modulated through solution immersion processes. For instance, a lignosulfonate-based hydrogel soaked in an  $\text{Fe}^{3+}$  solution not only effectively prevents the adhesion of pollutants but also exhibits strong adhesion to human skin.<sup>96</sup> Adhesion plays a critical role in the performance of sensor devices, while detection sensitivity is a key parameter for their evaluation. The hydrogel prepared by directly mixing 3-allyl-2-hydroxypropyl-lignin with polyacrylic acid exhibits high sensitivity to a range of pressure changes.<sup>115</sup> Incorporating metal nanoparticles into lignin-based hydrogels can significantly enhance their electrical conductivity. For example, adding silver nanoparticles to a hydrogel synthesized from lignin, acrylamide, and sodium alginate boosts its conductivity by approximately an order of magnitude.<sup>117</sup> Additionally, a novel nano-composite hydrogel based on lignin-modified MXene- $\text{Fe}^{3+}$  has been achieved. The integration of lignin-modified MXene (LM) and  $\text{Fe}^{3+}$  ions introduces a complex conductive network within the hydrogel, endowing it with unique electrical conductivity and strain-sensing capacity. As depicted in Fig. 6, this conductive hydrogel can detect both dynamic movements—such as running, walking, and jumping—and subtle physiological signals like facial/throat motion and breathing.<sup>118</sup> Such lignin-based hydrogels hold broad potential applications in areas, including self-adhesive strain sensors, wearable bioelectronics, and smartphone controllers.

Since lignin-based hydrogels possess a high water content, they are susceptible to freezing at temperatures below zero, resulting in compromised functional stability. Recent advancements in the development of freeze-resistant hydrogels have expanded their use in low-temperature environments. Adding

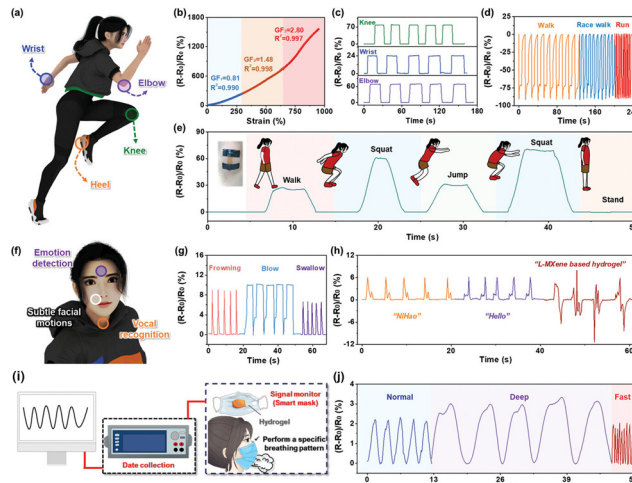


**Fig. 6** Sensing performance of lignin-based hydrogels.<sup>118</sup> (a) Schematic illustration of the hydrogel as a flexible sensor for human joint or motion detection. (b) The relative resistance variation  $((R - R_0)/R_0)$  of the hydrogel versus consecutively applied strain. Relative change in resistance response to (c) knee, wrist, and elbow bending, (d) different walking states, and (e) the movements of standing, squatting and jumping. (f) Schematic diagram for facial muscle and throat motion sensing. Real-time relative resistance changes in response to (g) different facial expressions and (h) different throat states. (i) Schematic illustration of a smart mask composed of the hydrogel and a wired transmission system. (j) Dynamic response curves of the smart mask to human breathing. [Reproduced from ref. 118 with permission from Elsevier, copyright of 2024.]

organic solvents and inorganic salts has been proven to effectively improve the freezing resistance of these hydrogels. For example, a lignin-based hydrogel sensor using a water/glycerin mixture as the dispersing medium and polyacrylic acid as the structural framework retains its sensitivity to detect limb movements, weak pulses, and throat vibrations even at low temperatures. This is attributed to the formation of robust hydrogen bonds between glycerin and water.<sup>80</sup> Additionally, introducing lithium chloride (LiCl) into the hydrogel improves its mechanical properties and electrical conductivity down to  $-30^\circ\text{C}$ . The hydrophobic interactions and filler effect of LiCl enable accurate monitoring and detection of human physiological activities in cold environments.<sup>93</sup> The development of frost-resistant hydrogels is a significant frontier in the ongoing research and innovation of lignin-based hydrogels, expanding their applicability and durability across various challenging conditions.

**3.2.2 Biomedical applications.** Lignin-based hydrogels have emerged as versatile candidates for wound dressings in biomedical applications. Wound dressings are a key strategy for managing and treating wounds. While traditional options like gauze and cotton balls offer some protection, they often tend to adhere to wounds and have limitations in clinical settings. Lignin-based hydrogels, with their biological functionality resembling living tissue, offer several advantages, including excellent antibacterial properties, mechanical strength, moist-

ure retention capabilities, and ease of cell adhesion. These features create an optimal environment that promotes wound healing. Additionally, their transparent or translucent nature allows for easy monitoring of the wound healing processes. For instance, a hydrogel synthesized from sulfoxylbetaine methacrylate and lignin methacrylate, with 40% lignin content, demonstrated impressive antibacterial properties, inhibiting *Escherichia coli* by 94.8% and *Staphylococcus aureus* by 95.7%, while supporting a cell survival rate of approximately 90%.<sup>82</sup>

Furthermore, the hydrogels' strong tissue adhesion and inherent softness make them effective for hemostatic applications, aiding in wound healing. As shown in Fig. 7a, a non-covalent reticulated lignosulfonate/polyvinylpyrrolidone complex hydrogel was applied to a punctured rat liver. The hydrogel's interaction with the damaged tissue enables stable adhesion to the bleeding site, serving as a protective layer that effectively prevents further bleeding, outperforming the conventional gauze pressing method.<sup>89</sup> Additionally, the notable conductivity of the Ag-LPA hydrogel composites within microfluidic-assisted hydrogel patches (MAHPs) was used to design a wound-healing patch (Fig. 7b). The MAHP group exhibited substantial wound recovery efficiency within 7 days, with visible scab formation.

Lignin-based hydrogels also possess a porous structure, making them ideal for drug incorporation. Depending on specific needs, drugs can be embedded in the hydrogel for a

slow and sustained release to the affected area, thereby facilitating wound healing. This is particularly useful when traditional administration routes, such as intravenous or oral delivery, are not feasible. In such cases, the drug-embedded hydrogel can be directly injected into the target site within the organism, enhancing the targeted therapeutic effect.

Recent advancements in lignin-based hydrogels have introduced additional biomedical functions. For example, the hydrogel synthesized from lignin and gelatin, crosslinked with glutaraldehyde, exhibits remarkable elasticity, fully recovering its shape after undergoing 90% compression and even allowing for injection *via* a syringe.<sup>102</sup> Lignin-based hydrogels doped with dual metals that exhibit pH-responsive properties can be utilized for laser-assisted antimicrobial photodynamic therapy, serving as targeted therapeutic agents for wound healing and related biomedical applications. These hydrogels can also be used to develop nano-coatings with stimulus-responsive antibacterial effects, offering broad potential in the biomedical field.<sup>75,79</sup>

**3.2.3 Energy storage.** The network structure of lignin-based hydrogels can be fine-tuned to create efficient ion transport channels, rendering them suitable for use as solid electrolytes in energy storage systems. These assembled supercapacitors usually exhibit higher power density, better charge and discharge efficiency, and better cycling performance. Moreover, due to the hydrogels' inherent absorption capabilities, they mitigate issues like liquid leakage and combustion—common problems with traditional liquid electrolytes, thereby enhancing the overall safety of the energy system.<sup>119</sup> A series of lignin-based hydrogels with varying crosslinking degrees have been employed as semi-solid electrolytes. These hydrogels are typically prepared using kraft lignin and polyethylene glycol diglycidyl ether as a crosslinking agent. When assembled with polyaniline@carbon cloth flexible electrodes, the resulting textile-based supercapacitors demonstrate excellent ionic conductivity and rate capabilities. Notably, they maintain high capacitance and coulombic efficiency even after repeated charge-discharge cycles.<sup>85,97</sup> Incorporating metal ions can further enhance the ion transport capacity of these electrolytes. For example, supercapacitors formed by introducing  $\text{Fe}^{3+}$  into lignin-based hydrogels achieve a high capacitance, with a remarkable capacitance retention rate of 94.1% after 10 000 consecutive charge-discharge cycles. Lignin-based hydrogels can also serve as ideal electrode materials.<sup>88</sup> By integrating a lignin hydrogel electrolyte with electrospun lignin/polyacrylonitrile nanofiber electrodes, an all-lignin-based flexible supercapacitor can be produced,<sup>74</sup> exhibiting excellent electrochemical performances.

Given their excellent water absorption and ion transport capabilities, lignin-based hydrogels hold significant potential for applications in the field of wet gas power generation. For example, Zhang *et al.*<sup>84</sup> synthesized hydrogels with a polyvinyl alcohol (PVA) rigid skeleton and lignin as the intensifier. The incorporation of lignin into the hydrogel significantly enhances its pH responsiveness, mechanical strength, and wet power generation performance (Fig. 8c and d). When subjected

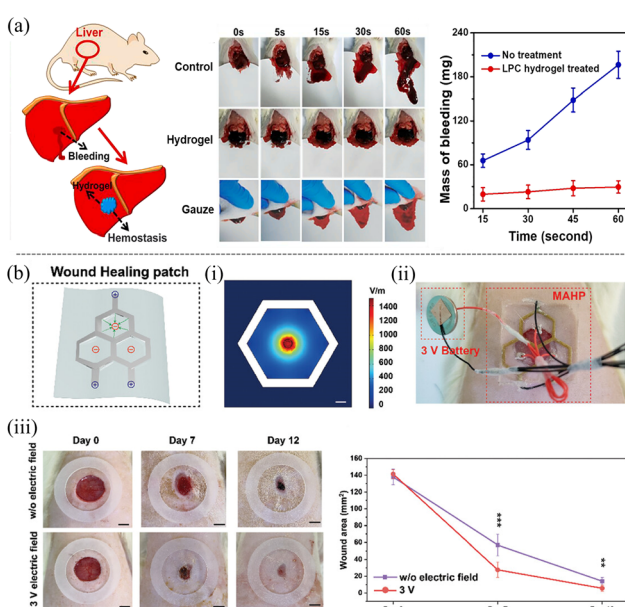


**Fig. 7** Application of lignin-based hydrogels in (a) hemostatic applications<sup>89</sup> and (b) wound healing.<sup>106</sup> (i) Voltage stimulation of the wound healing microfluidic-assisted hydrogel patches (MAHPs). Scale bar = 1 mm. (ii) Demonstration of MAHP covered on the wound of a Sprague-Dawley (SD) rat. (iii) Optical images of wound areas on various days. [Reproduced from ref. 89 with permission from Elsevier, copyright of 2022.] [Reproduced from ref. 106 with permission from Wiley, copyright of 2024.]

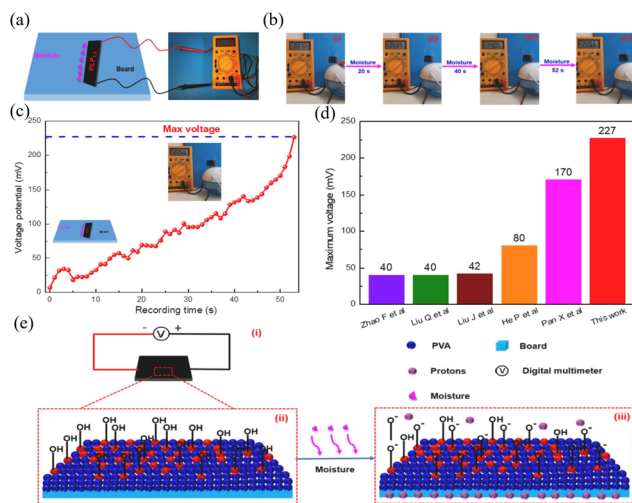


**Fig. 8** (a) Schematic diagram of the lignin reinforced PVA hydrogel-based moist-electric generator (LRP-HMEG) and (b) voltage output of LRP-HMEG under continuous moisture flow. (c) The effect of moisture duration on voltage. (d) Comparison of electric power generation of LRP-HMEG and other moist-electric generators. (e) Mechanism of the moist-electric generator.<sup>84</sup> [Reproduced from ref. 84 with permission from Elsevier, copyright of 2021.]

to a high-humidity environment, lignin and PVA within the hydrogels release a significant number of protons, which rapidly migrate from one side to the other (as depicted in Fig. 8e, iii), thereby generating an output voltage. The incorporation of metal ions into hydrogels can also enhance their conductivity, which in turn significantly improves their power generation performance. For instance, a polyacrylic acid ionic hydrogel synthesized using a lignosulfonate-Al<sup>3+</sup> composite system delivers an open-circuit voltage of up to 550 mV in an environment with 55% relative humidity. This voltage is generated due to the water content disparity between the top and bottom surfaces of the hydrogel, creating an ion concentration gradient that drives the migration of H<sup>+</sup> ions, inducing a potential across the external circuit.<sup>98</sup> These innovative applications of lignin-based hydrogels highlight their versatility and potential in advancing sustainable energy technologies.

**3.2.4 Adsorption application.** The porous structure of lignin-based hydrogels renders them effective for the adsorption of organic pollutants and inorganic ions, making them a promising material for adsorption applications. For example, the lignin/cellulose hydrogel, composed of sodium lignosulfonate, cellulose and 0.1% acetic acid solution, has demonstrated adsorption capacities of 294.0 mg g<sup>-1</sup> for Congo red and 129.8 mg g<sup>-1</sup> for malachite green.<sup>99</sup> A lignin-PVA superabsorbent hydrogel, using biomass lignin as the raw material, PVA as the matrix template and epichlorohydrin as the cross-linking agent, has shown adsorption capacities of 196 mg g<sup>-1</sup> for rhodamine 6G, 169 mg g<sup>-1</sup> for Gentian Violet and 179 mg g<sup>-1</sup> for methylene blue dyes, respectively.<sup>120</sup>

Leveraging the functional groups present in lignin, chemical modifications such as alkylation, hydroxymethylation,

alkylation oxidation, and sulfonation have been employed to regulate the spatial network structure of lignin, thereby obtaining lignin-based adsorbents with enhanced adsorption properties. For example, a bio-based hydrogel (LN-NH-SA), made from ammoniated lignin and sodium alginate, exhibits a remarkable adsorption effect on methyl blue, with a maximum adsorption capacity of 388.81 mg g<sup>-1</sup>, making it a bio-based adsorbent with high adsorption capacity.<sup>83</sup> Grafting acrylic acid and 2-acrylamide-2-methyl-propanesulfonic acid onto the lignin structure, along with the addition of bentonite, results in a lignin composite hydrogel with excellent dye-adsorption properties. The adsorption capacities of this hydrogel for malachite green, methyl blue, and rhodamine B are 2541.76 mg g<sup>-1</sup>, 1284.46 mg g<sup>-1</sup>, and 1047.72 mg g<sup>-1</sup>, respectively.<sup>101</sup> An alkaline nucleophilic substitution reaction has been used to chemically modify sulfate lignin and functionalize it. Metal ion adsorption experiments conducted on the synthesized active hydrogel showed adsorption rates of Pb<sup>2+</sup> and Cu<sup>2+</sup> higher than 90% and 80%, respectively.<sup>78</sup> Recently, a novel lignosulfonate modified graphene hydrogel has been developed for the removal of Cr<sup>4+</sup> from aqueous solutions, with an adsorption capacity of up to 1743.9 mg g<sup>-1</sup>.<sup>121</sup>

Beyond the previously mentioned applications, lignin-based hydrogels have potential use in intelligent switching systems, pollutant degradation, and plant protection.<sup>81,91,95</sup> The unique structural attributes of lignin-based hydrogels allow for broad applications. By systematically developing the structural features of hydrogels and exploring innovative modification methods, the scope of their applications across various fields can be further expanded.

## 4. Lignin-based adhesives

China is a leading producer of wood-based panels globally.<sup>122</sup> The traditional adhesives for wood-based panels mainly include urea-formaldehyde resin, phenolic resin, and melamine-formaldehyde resin, as well as their modified derivatives.<sup>123,124</sup> The production of these adhesives relies heavily on non-renewable fossil resources and formaldehyde, which are detrimental to natural resources, environmental sustainability, and human health.<sup>125–128</sup> Facing the increasing demand for wood adhesives, there is a growing preference for adhesives derived from renewable resources.<sup>129</sup> Lignin, a natural adhesive in plants, strengthens the cell wall by binding cellulose and hemicellulose fibers together.<sup>20</sup> Its inherent properties enable it to replace phenol in adhesive formulations and to act as a modifier, reducing the emission of free formaldehyde or phenol in the final products.<sup>130,131</sup> Therefore, lignin is a promising candidate for the development of eco-friendly wood adhesives.

In the synthesis of lignin-based adhesives, lignin can be employed as a primary constituent or an auxiliary material. As a primary material, lignin can be utilized in its raw form or serve as a substitute for phenol in adhesive formulations.<sup>127,128</sup> By treating the bamboo matrix with NaOH solution, some

lignin and hemicellulose are removed, and upon hot pressing, the bamboo fibers are compressed into a dense structure, creating an *in situ* bonded bamboo material.<sup>20</sup> The interplay of hydrogen bonds and physical entanglements within the lignin/cellulose composite results in a high bonding strength of  $4.4 \pm 0.3$  MPa for *in situ* bonded bamboo. Chemically treated bamboo, when mixed with alkaline lignin, polypropylene glycol bis(2-aminopropylether), and wood flour, forms particleboard through hot pressing. This lignin-based adhesive not only emits low levels of formaldehyde but also provides excellent internal bonding strength due to its network of ionic and covalent bonds.<sup>132</sup> Lignin that is non-condensed or slightly condensed, obtained through biomass separation technology, can be directly used as an adhesive for plywood when mixed with water.<sup>133</sup> This lignin-based adhesive can produce high-performance plywood over a wide range of hot pressing temperatures, and its adhesive performance can be further optimized by adjusting the hot pressing process parameters, as shown in Fig. 9. Meanwhile, lignin can effectively replace phenol in the preparation of wood adhesives, significantly reducing the content of free phenol and free formaldehyde, ensuring that the material possesses good mechanical properties. Industrial lignin, obtained from various lignocellulosic biomasses, can also be used in wood adhesive formulations. A lignin-based wood adhesive has been developed through the hydrodeoxygenation and acid-mediated methylation of industrial lignin. This novel adhesive is not only phenol-free but also exhibits a lighter color and superior bonding properties.<sup>134</sup>

Lignin, when utilized as an auxiliary material, is primarily integrated with other components to prepare wood adhesives. Studies have shown that lignin can effectively reduce the presence of free formaldehyde, enhance water resistance, and endow the adhesive with superior thermal stability and mechanical properties. Specifically, a lignin-based adhesive,

synthesized from a mixture of lignin and acrylic acid in *N,N*-dimethylformamide under alkaline conditions, demonstrates remarkable internal bonding strength across a spectrum of pH environments, including neutral, acidic, and alkaline settings.<sup>32</sup> Further exploration into the influence of the proportion and particle size of kraft lignin on the adhesion properties of soybean protein adhesive has revealed that the addition of lignin improves the viscosity, dispersibility and thermal stability of soybean protein adhesive. Notably, the wet adhesion strength is observed to increase with a decrease in the particle size of lignin, indicating a refined approach for adhesive formulation for improved performance.<sup>135</sup>

Chemical modification of lignin enhances its chemical reactivity and compatibility, substantially reducing formaldehyde emissions in lignin-modified adhesives and endowing them with desirable mechanical properties. For example, a formaldehyde-free lignin-based adhesive, prepared with aminated alkali lignin-Cu nanoparticles, has exhibited a remarkable bonding strength of 1.51 MPa and a debonding work of 0.272 J. These values are 2.75 and 6.33 times higher, respectively, than those of the unmodified lignin adhesive. Such enhancements are attributed to the dense crosslinked network within the adhesive, a result of the synergistic effects of covalent, coordination, and hydrogen bonding, as well as the unique structure of the hyperbranched polymer (Fig. 10a).<sup>136</sup> When alkali lignin is dispersed in an alkaline chloride DES and heated to 90 °C for 12 hours, lignin depolymerization occurs, characterized by the cleavage of ether bonds and demethoxylation, which leads to the formation of phenolic hydroxyl groups and alcoholic hydroxyl groups, increasing the reactive sites of lignin. Meanwhile, the particle size of lignin also decreases from 205.6 nm to 44.3 nm. Upon the subsequent addition of furfural, a lignin-furfural composite adhesive is produced. The adhesive achieves a bonding strength of up to 5.71 MPa on paulownia wood boards, outperforming that of other reported lignin-based adhesives, which typically exhibit a bonding strength of 1–4 MPa.<sup>137,138</sup> In the preparation process, lignin and furfural entirely replace the conventional phenol and formaldehyde in the presence of DES and hence the adhesive is a kind of composite product formed of DES, lignin and furfural, demonstrating its potential as an ideal substitute for phenolic and urea-formaldehyde adhesives.<sup>139</sup>

The development of multifunctional bio-adhesives plays a critical role in achieving a sustainable society. In a recent study, a bio-based adhesive with a triple network structure was synthesized by mixing lignin, copper ions, and soy protein isolate. The quinone groups of lignin cross-link with the amino groups in soy protein, ensuring the adhesive's binding strength and water resistance. The catechol structures formed by lignin demethylation enhance the toughness and coating performance of the adhesive through hydrogen bond networks. Multifunctional copper ions form multiple interfacial coordination bonds, which reduce the adhesive's viscosity and significantly improve its toughness and coating properties.<sup>141</sup> Furthermore, a tough adhesive composed of a lignin polyurea (LPU) framework and soybean protein (SP) is developed. The

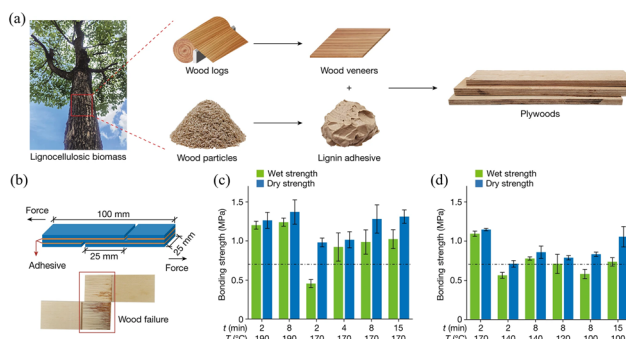


**Fig. 9** (a) Schematic illustration of the preparation of plywood from wood veneers with lignin as adhesives. (b) Schematic illustration of three-layer formaldehyde-protected lignin (FPL)-bonded plywood specimens used for adhesion performance tests (top) and wood failure of the specimen after a wet strength test (bottom). (c) Effects of hot-pressing temperatures and times on the adhesion performance of FPL adhesives. (d) The promotion effect of acid addition on the adhesion performances of FPL adhesives.<sup>133</sup> [Reproduced from ref. 133 with permission from Springer Nature, copyright of 2023.]

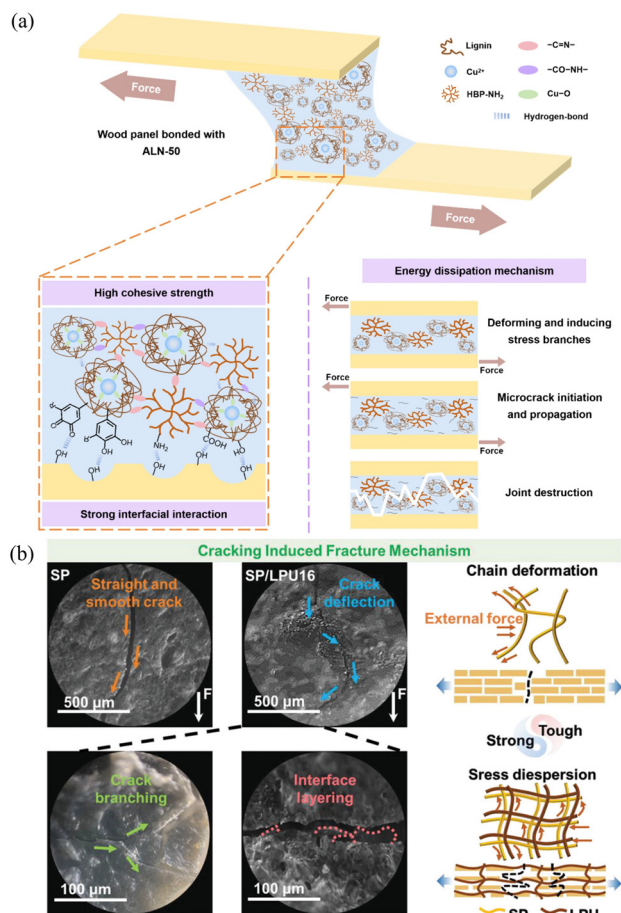


**Fig. 10** (a) Strengthening and toughening mechanism of a lignin-based adhesive.<sup>136</sup> [Reproduced from ref. 136 with permission from Elsevier, copyright of 2024.] (b) Cross-sectional analysis of an SP-based adhesive for fracture.<sup>140</sup> [Reproduced from ref. 140 with permission from Wiley, copyright of 2024.]

LPU framework serves as rigid nervures to slow crack propagation and distribute stress, while the SP dissipates the strain energy through the interaction of the graded hydrogen and imine bonds between LPU and SP, as shown in Fig. 10b. Compared with SP, the fracture toughness and water resistance of this bio-adhesive are significantly improved by approximately 7 times and 23 times, respectively. The dynamic network of the adhesive facilitates effective diffusion and rearrangement at the interface, providing excellent recyclability and reprocessability.<sup>140</sup> This pioneering approach for adhesive formulation highlights the versatile application of lignin and its capacity to transform the adhesive industry with eco-friendly and high-performance solutions. Finally, the adhesion performance is an important metric for evaluating the quality of adhesives. The adhesion strength of commercially available phenolic resin adhesives typically falls in the range of 1–20 MPa.<sup>142</sup> In comparison, the adhesion strength of lignin-based adhesives varies within the range of 1–13 MPa.<sup>126,143</sup> Therefore, the adhesion performance of lignin-based adhesives requires further optimization.

## 5. Conclusion and prospect

Lignin, the most abundant renewable source of aromatic compounds in nature, exhibits the advantages of cost-effectiveness, remarkable antibacterial properties, high mechanical strength, and bio-environmental friendliness. The burgeoning field of lignin-based materials, particularly hydrogels and adhesives, has become a hot topic of research in recent years due to their excellent functional properties and broad applications. This article begins by describing the structure of lignin and then provides a detailed review of the preparation methods and application fields of these two types of materials.

Lignin-based hydrogels exhibit good biocompatibility, biodegradability, antioxidant and antibacterial properties. Despite their potential being extensively studied in flexible sensing, biomedicine, energy storage and adsorption, certain challenges remain. First of all, the biomedical application of lignin-based hydrogels needs further investigation. Considering the importance of safety in food and pharmaceutical industries, and the relative scarcity of research on lignin's safety profile, there is an urgent need for a comprehensive and systematic assessment of the toxicity of different lignin structures. Establishing a standardized detection and quantification system is crucial for ensuring the secure biomedical application of lignin-based hydrogels. Secondly, expanding the types of lignin used in hydrogel formulation and exploring the correlation between the lignin structure and hydrogel properties will substantially improve the synthesis process and optimize the hydrogel performance. Given lignin's diversity and structural complexity, leveraging high-performance machine learning techniques to precisely predict material properties is key to advancing the future development of lignin-based hydrogel materials.

Compared to hydrogels, the research of lignin-based adhesives is still in its infancy. Existing studies have demonstrated the potential of lignin in producing high-performance wood adhesives, which not only reduce the manufacturing cost but also mitigate environmental pollution. For example, substituting 60% of phenol with demethylated lignin in adhesive formation results in a reduction of formaldehyde emission to  $0.059 \text{ mg m}^{-3}$ , satisfying the E<sub>1</sub> grade, and also a 28.48% decrease in volatile organic compound emissions compared to phenol formaldehyde plywood.<sup>144</sup> However, future advancements in this field demand more systematic and comprehensive research endeavors. On the one hand, there is a pressing need to discover greener and easier synthesis techniques. Efforts should be directed towards reducing the reliance on toxic and harmful chemicals, such as formaldehyde, with the goal of developing entirely eco-friendly adhesive products. On the other hand, the properties of lignin-based adhesives require further improvement. Compared with fossil-based adhesives, the current lignin-based adhesives display inferior adhesion performance, which is the primary obstacle to their widespread adoption. The key lies in striking a balance between environmental sustainability and performance efficacy, thereby paving the way for the industrial application of lignin-based adhesives.

## Data availability

No primary research results, software or code have been included and no new data were generated or analyzed as part of this review.

## Conflicts of interest

There are no conflicts to declare.

## Acknowledgements

This work was supported by the National Key Research and Development Program of China (2021YFB3802600), the National Natural Science Foundation of China (22278396, 22378392, 22338007, 22208344), the Youth Innovation Promotion Association CAS (Y2021022), and the Open Research Fund of State Key Laboratory of Mesoscience and Engineering (MESO-23-D17). The authors sincerely appreciate Prof. Suojiang Zhang (IPE, CAS) for his careful academic guidance and great support.

## References

- 1 T. Wang, H. Li, X. Diao, X. Lu, D. Ma and N. Ji, *Ind. Crops Prod.*, 2023, **199**, 116715–116736.
- 2 Y. Qin, Y. Chen, X. Zeng, Y. Liu, X. Lin, W. Zhang and X. Qiu, *Green Energy Environ.*, 2023, **8**, 1728–1736.
- 3 Y. Zhu, Z. Li and J. Chen, *Green Energy Environ.*, 2019, **4**, 210–244.
- 4 S. Kant Bhatia, A. K. Palai, A. Kumar, R. Kant Bhatia, A. Kumar Patel, V. Kumar Thakur and Y.-H. Yang, *Bioresour. Technol.*, 2021, **340**, 125644–125655.
- 5 J. Fu, F. Shen, X. Liu and X. Qi, *Green Energy Environ.*, 2023, **8**, 842–851.
- 6 X. Wang, S. Feng, Y. Wang, Y. Zhao, S. Huang, S. Wang and X. Ma, *Green Energy Environ.*, 2023, **8**, 927–937.
- 7 G. Liu, Z. Zhai, Y. Lu, J. Lu, Y. Wang, S. Liang, H. He and L. Jiang, *Chem. Bio. Eng.*, 2024, **1**, 357–365.
- 8 B. Qiu, X. Tao, J. Wang, Y. Liu, S. Li and H. Chu, *Energy Convers. Manage.*, 2022, **261**, 115647–115674.
- 9 J. de Aguiar, T. J. Bondancia, P. I. C. Claro, L. H. C. Mattoso, C. S. Farinas and J. M. Marconcini, *ACS Sustainable Chem. Eng.*, 2020, **8**, 2287–2299.
- 10 W. Deng, Y. Feng, J. Fu, H. Guo, Y. Guo, B. Han, Z. Jiang, L. Kong, C. Li, H. Liu, P. T. T. Nguyen, P. Ren, F. Wang, S. Wang, Y. Wang, Y. Wang, S. S. Wong, K. Yan, N. Yan, X. Yang, Y. Zhang, Z. Zhang, X. Zeng and H. Zhou, *Green Energy Environ.*, 2023, **8**, 10–114.
- 11 Y. Zhang, H. He, Y. Liu, Y. Wang, F. Huo, M. Fan, H. Adidharma, X. Li and S. Zhang, *Green Chem.*, 2019, **21**, 9–35.
- 12 X. Liu, X. Duan, W. Wei, S. Wang and B.-J. Ni, *Green Chem.*, 2019, **21**, 4266–4289.
- 13 S. Chakraborty and S. K. Paul, *Curr. Opin. Chem. Eng.*, 2020, **29**, 104–121.
- 14 J. Zhang, *Green Energy Environ.*, 2018, **3**, 328–334.
- 15 G. Liu, Q. Wang, D. Yan, Y. Zhang, C. Wang, S. Liang, L. Jiang and H. He, *Green Chem.*, 2021, **23**, 1665–1677.
- 16 S. Farooq Adil, V. S. Bhat, K. M. Batoo, A. Imran, M. E. Assal, B. Madhusudhan, M. Khan and A. Al-Warthan, *J. Saudi Chem. Soc.*, 2020, **24**, 374–379.
- 17 J. Yuan, G. Du, H. Yang, S. Liu, S. Park, T. Liu, X. Ran, B. D. Park, W. Gao and L. Yang, *Ind. Crops Prod.*, 2023, **204**, 117279–117288.
- 18 Y. Ma, Z. Jiang, Y. Luo, X. Guo, X. Liu, Y. Luo and B. Shi, *Green Energy Environ.*, 2024, **9**, 597–603.
- 19 X. Zhao, Y. Zhang, H. Hu, Z. Huang, M. Yang, D. Chen, K. Huang, A. Huang, X. Qin and Z. Feng, *Int. J. Biol. Macromol.*, 2016, **91**, 1081–1089.
- 20 X. Li, Y. Meng, Z. Cheng and B. Li, *Polymers*, 2023, **15**, 3372–3388.
- 21 J. Mu, C. Li, J. Zhang, X. Song, S. Chen and F. Xu, *Green Energy Environ.*, 2023, **8**, 1479–1487.
- 22 L. Dai, R. Liu, L.-Q. Hu, Z.-F. Zou and C.-L. Si, *ACS Sustainable Chem. Eng.*, 2017, **5**, 8241–8249.
- 23 Z. Chen, J. Luo, Y. Hu, Y. Fu, J. Meng, S. Luo, L. Wang, Y. Zhang, J. Zhou, M. Zhang and H. Qin, *Int. J. Biol. Macromol.*, 2022, **222**, 487–496.
- 24 G. Jia, M. T. Innocent, Y. Yu, Z. Hu, X. Wang, H. Xiang and M. Zhu, *Int. J. Biol. Macromol.*, 2023, **226**, 646–659.
- 25 S. Wang, Y. Yuan, T.-Q. Yuan and X. Wang, *Green Chem.*, 2023, **25**, 4013–4021.
- 26 X. Gong, T. Liu, S. Yu, Y. Meng, J. Lu, Y. Cheng and H. Wang, *Ind. Crops Prod.*, 2020, **153**, 112593–112596.
- 27 Q. Li, M. T. Naik, H.-S. Lin, C. Hu, W. K. Serem, L. Liu, P. Karki, F. Zhou and J. S. Yuan, *Carbon*, 2018, **139**, 500–511.
- 28 C. Huang, J. Ma, W. Zhang, G. Huang and Q. Yong, *Polymers*, 2018, **10**, 841–852.
- 29 N. Tahari, P. L. de Hoyos-Martinez, M. Abderrabba, S. Ayadi and J. Labidi, *Colloids Surf., A*, 2020, **602**, 125108–125117.
- 30 K. Ganie, M. A. Manan, A. Ibrahim and A. K. Idris, *Int. J. Chem. Eng.*, 2019, 1–6, DOI: [10.1155/2019/4120859](https://doi.org/10.1155/2019/4120859).
- 31 L. Cui, Y. An, H. Xu, M. Jia, Y. Li and X. Jin, *New J. Chem.*, 2021, **45**, 21692–21700.
- 32 S. K. Singh, K. Ostendorf, M. Euring and K. Zhang, *Green Chem.*, 2022, **24**, 2624–2635.
- 33 L. Dong, L. Lin, X. Han, X. Si, X. Liu, Y. Guo, F. Lu, S. Rudić, S. F. Parker, S. Yang and Y. Wang, *Chem.*, 2019, **5**, 1521–1536.
- 34 G. Liu, Y. Lu, J. Lu, Y. Wang, S. Liang, H. He and L. Jiang, *Nano Res.*, 2023, **17**, 2420–2428.
- 35 H. Guo, B. Zhang, C. Li, C. Peng, T. Dai, H. Xie, A. Wang and T. Zhang, *ChemSusChem*, 2016, **9**, 3220–3229.
- 36 Y. Hu, L. Yan, X. Zhao, C. Wang, S. Li, X. Zhang, L. Ma and Q. Zhang, *Green Chem.*, 2021, **23**, 7030–7040.
- 37 S. Wang, J. Bai, M. T. Innocent, Q. Wang, H. Xiang, J. Tang and M. Zhu, *Green Energy Environ.*, 2022, **7**, 578–605.

38 T. Aro and P. Fatehi, *ChemSusChem*, 2017, **10**, 1861–1877.

39 M. V. Galkin and J. S. M. Samec, *ChemSusChem*, 2016, **9**, 1544–1558.

40 S. Laurichesse and L. Avérous, *Prog. Polym. Sci.*, 2014, **39**, 1266–1290.

41 Y. Meng, J. Lu, Y. Cheng, Q. Li and H. Wang, *Int. J. Biol. Macromol.*, 2019, **135**, 1006–1019.

42 Z. Wang and P. J. Deuss, *Biotechnol. Adv.*, 2023, **68**, 108230–108251.

43 P. Gu, W. Liu, Q. Hou and Y. Ni, *J. Mater. Chem. A*, 2021, **9**, 14233–14264.

44 M. Zhang, R. Tian, S. Tang, K. Wu, B. Wang, Y. Liu, Y. Zhu, H. Lu and B. Liang, *Int. J. Biol. Macromol.*, 2023, **243**, 125219–125228.

45 C. Li, X. Zhao, A. Wang, G. W. Huber and T. Zhang, *Chem. Rev.*, 2015, **115**, 11559–11624.

46 C. Zhao, Z. Hu, L. Shi, C. Wang, F. Yue, S. Li, H. Zhang and F. Lu, *Green Chem.*, 2020, **22**, 7366–7375.

47 J. Ou, S. Hu, L. Yao, Y. Chen, H. Qi and F. Yue, *Chem. Eng. J.*, 2023, **453**, 139770–139780.

48 R. D'Orsi, C. V. Irimia, J. J. Lucejko, B. Kahraman, Y. Kanbur, C. Yumusak, M. Bednorz, F. Babudri, M. Irimia-Vladu and A. Operamolla, *Adv. Sustainable Syst.*, 2022, **6**, 2200285–2200298.

49 S. Guadix-Montero and M. Sankar, *Top. Catal.*, 2018, **61**, 183–198.

50 A. Eraghi Kazzaz and P. Fatehi, *Ind. Crops Prod.*, 2020, **154**, 112732–112744.

51 C. Zhang, X. Shen, Y. Jin, J. Cheng, C. Cai and F. Wang, *Chem. Rev.*, 2023, **123**, 4510–4601.

52 D. S. Bajwa, G. Pourhashem, A. H. Ullah and S. G. Bajwa, *Ind. Crops Prod.*, 2019, **139**, 111526–111536.

53 H. Sadeghifar and A. Ragauskas, *ACS Sustainable Chem. Eng.*, 2020, **8**, 8086–8101.

54 L. K. S. Gujjala, J. Kim and W. Won, *J. Cleaner Prod.*, 2022, **363**, 132585–132303.

55 X. Ouyang, X. Qiu, H. Lou and D. Yang, *Ind. Eng. Chem. Res.*, 2006, **45**, 5716–5721.

56 H. S. Arel and E. Aydin, *Adv. Sustainable Syst.*, 2017, **157**, 1084–1091.

57 C. Liu, Y. Li, J. Zhuang, Z. Xiang, W. Jiang, S. He and H. Xiao, *Polymers*, 2022, **14**, 3739–3757.

58 X. Zhao, K. Cheng and D. Liu, *Appl. Microbiol. Biotechnol.*, 2009, **82**, 815–827.

59 A. Sakakibara, *Wood Sci. Technol.*, 1980, **14**, 89–100.

60 G. Zinov'yev, I. Sumerskii, T. Rosenau, M. Balakshin and A. Potthast, *Molecules*, 2018, **23**, 2223–2232.

61 A. Björkman, *Nature*, 1954, **174**, 1057–1058.

62 J. S. Luterbacher, A. Azarpira, A. H. Motagamwala, F. Lu, J. Ralph and J. A. Dumesic, *Energy Environ. Sci.*, 2015, **8**, 2657–2663.

63 Z. Chen, X. Bai, L. A and C. Wan, *ACS Sustainable Chem. Eng.*, 2018, **6**, 12205–12216.

64 J.-Y. Kim, E.-J. Shin, I.-Y. Eom, K. Won, Y. H. Kim, D. Choi, I.-G. Choi and J. W. Choi, *Bioresour. Technol.*, 2011, **102**, 9020–9025.

65 F. Hong, P. Qiu, Y. Wang, P. Ren, J. Liu, J. Zhao and D. Gou, *Food Chem.:X*, 2024, **21**, 101095–101109.

66 Q. Xu, J. E. Torres, M. Hakim, P. M. Babiak, P. Pal, C. M. Battistoni, M. Nguyen, A. Panitch, L. Solorio and J. C. Liu, *Mater. Sci. Eng., R*, 2021, **146**, 100641–100738.

67 S. Afewerki, X. Wang, G. U. Ruiz-Esparza, C.-W. Tai, X. Kong, S. Zhou, K. Welch, P. Huang, R. Bengtsson, C. Xu and M. Strømme, *ACS Nano*, 2020, **14**, 17004–17017.

68 X. Han, Y. Su, G. Che, J. Zhou and Y. Li, *ACS Sustainable Chem. Eng.*, 2023, **11**, 8255–8270.

69 S. Huang, S. Shuyi, H. Gan, W. Linjun, C. Lin, X. Danyuan, H. Zhou, X. Lin and Y. Qin, *Carbohydr. Polym.*, 2019, **223**, 115080–115086.

70 H. Cui, W. Jiang, C. Wang, X. Ji, Y. Liu, G. Yang, J. Chen, G. Lyu and Y. Ni, *Composites, Part B*, 2021, **225**, 109316–109327.

71 X. Han, Y. Zhang, F. Ran, C. Li, L. Dai, H. Li, F. Yu, C. Zheng and C. Si, *Ind. Crops Prod.*, 2022, **176**, 114366–114374.

72 Y. Chen, K. Zheng, L. Niu, Y. Zhang, Y. Liu, C. Wang and F. Chu, *Int. J. Biol. Macromol.*, 2019, **128**, 414–420.

73 Y. Dou, X. Wang, Z. Liu, F. Kong and S. Wang, *J. Appl. Polym. Sci.*, 2023, **141**, e54910.

74 J. H. Park, H. H. Rana, J. Y. Lee and H. S. Park, *J. Mater. Chem. A*, 2019, **7**, 16962–16968.

75 K. Ravishankar, M. Venkatesan, R. P. Desingh, A. Mahalingam, B. Sadhasivam, R. Subramaniyam and R. Dhamodharan, *Mater. Sci. Eng., C*, 2019, **102**, 447–457.

76 W. Yang, F. Xu, X. Ma, J. Guo, C. Li, S. Shen, D. Puglia, J. Chen, P. Xu, J. Kenny and P. Ma, *Mater. Sci. Eng., C*, 2021, **129**, 112385–112394.

77 G. Yan, S. He, G. Chen, S. Ma, A. Zeng, B. Chen, S. Yang, X. Tang, Y. Sun, F. Xu, L. Lin and X. Zeng, *Nano-Micro Lett.*, 2022, **14**, 84–97.

78 D. Rico-García, L. G. Guerrero-Ramírez, L. R. Cajero-Zul, E. Orozco-Guareño, E. B. Figueroa-Ochoa, R. A. Gutiérrez-Saucedo, L. Pérez-Alvarez, J. L. Vilas-Vilela and S. L. Hernandez-Olmos, *Appl. Sci.*, 2021, **11**, 4012–4025.

79 S. Chandna, N. S. Thakur, R. Kaur and J. Bhaumik, *Biomacromolecules*, 2020, **21**, 3216–3230.

80 Q. Wang, X. Pan, C. Lin, D. Lin, Y. Ni, L. Chen, L. Huang, S. Cao and X. Ma, *Chem. Eng. J.*, 2019, **370**, 1039–1047.

81 L. Dai, M. Ma, J. Xu, C. Si, X. Wang, Z. Liu and Y. Ni, *Chem. Mater.*, 2020, **32**, 4324–4330.

82 C. Xu, L. Liu, S. Renneckar and F. Jiang, *Ind. Crops Prod.*, 2021, **170**, 113759–113768.

83 C. Wang, X. Feng, S. Shang, H. Liu, Z. Song and H. Zhang, *Int. J. Biol. Macromol.*, 2023, **237**, 124200–124210.

84 Y. Zhang, A. MohebbiPour, J. Mao, J. Mao and Y. Ni, *Int. J. Biol. Macromol.*, 2021, **193**, 941–947.

85 Y. Fei, Z. Jiang, D. Zhou, F. Meng, Y. Wu, Y. Xiong, Y. Ye, T. Liu, Z. Fei, T. Kuang, M. Zhong, Y. Li and F. Chen, *J. Energy Storage*, 2023, **73**, 108978–108985.

86 Y. Zhang, M. Jiang, Y. Zhang, Q. Cao, X. Wang, Y. Han, G. Sun, Y. Li and J. Zhou, *Mater. Sci. Eng., C*, 2019, **104**, 110002–110009.

87 Y. Chao, S. Yu, H. Zhang, D. Gong, J. Li, F. Wang, J. Chen, J. Zhu and J. Chen, *ACS Appl. Bio Mater.*, 2023, **6**, 1525–1535.

88 A. K. Mondal, D. Xu, S. Wu, Q. Zou, F. Huang and Y. Ni, *Biomacromolecules*, 2022, **23**, 766–778.

89 J. Cao, Y. Zhao, S. Jin, J. Li, P. Wu and Z. Luo, *Chem. Eng. J.*, 2022, **429**, 132252–132263.

90 L. Jiang, J. Liu, S. He, A. Liu, J. Zhang, H. Xu and W. Shao, *Chem. Eng. J.*, 2022, **430**, 132653–132663.

91 J. Tan, J. Wang, Z. Tan, M. Yu, Z. Yang, Z. Ren, Y. Li, Y. Zhang and X. Lin, *Chem. Eng. J.*, 2023, **451**, 138504–138522.

92 Q. Wang, X. Pan, C. Lin, X. Ma, S. Cao and Y. Ni, *Chem. Eng. J.*, 2020, **396**, 125341–125349.

93 Y. Zhang, J. Mao, W. Jiang, S. Zhang, L. Tong, J. Mao, G. Wei, M. Zuo and Y. Ni, *Composites, Part B*, 2021, **217**, 108879–108887.

94 A. K. Mondal, S. Wu, D. Xu, Q. Zou, L. Chen, L. Huang, F. Huang and Y. Ni, *Int. J. Biol. Macromol.*, 2021, **187**, 189–199.

95 B. Song, H. Liang, R. Sun, P. Peng, Y. Jiang and D. She, *Int. J. Biol. Macromol.*, 2020, **144**, 219–230.

96 Q. Wang, J. Lan, Z. Hua, X. Ma, L. Chen, X. Pan, Y. Li, S. Cao and Y. Ni, *Int. J. Biol. Macromol.*, 2021, **184**, 282–288.

97 Q. Wu, C. Jiang, S. Zhang, S. Yu and L. Huang, *J. Mater. Chem. A*, 2022, **10**, 16853–16865.

98 J. Zhang, J. Zhuang, L. Lei and Y. Hou, *J. Mater. Chem. A*, 2023, **11**, 3546–3555.

99 X. Li, P. Li, W. Chen, J. Ren and W. Wu, *Materials*, 2023, **16**, 4260–4274.

100 C. Fu, X. Liu, Y. Yi, P. Fatehi, X. Meng, F. Kong and S. Wang, *Polym. Test.*, 2022, **107**, 107486–107493.

101 M. Jiang, N. Niu and L. Chen, *Sep. Purif. Technol.*, 2022, **285**, 120376–120390.

102 T. Abdullah, T. Colombani, T. Alade, S. A. Bencherif and A. Memić, *Biomacromolecules*, 2021, **22**, 4110–4121.

103 K. Rajan, J. K. Mann, E. English, D. P. Harper, D. J. Carrier, T. G. Rials, N. Labb   and S. C. Chmely, *Biomacromolecules*, 2018, **19**, 2665–2672.

104 P. Deng, F. Chen, H. Zhang, Y. Chen and J. Zhou, *ACS Appl. Mater. Interfaces*, 2021, **13**, 52333–52345.

105 C. Chen, N. Zheng, W. Wu, M. Tang, W. Feng, W. Zhang, X. Li, Y. Jiang, J. Pang, D. Min and L. Fu, *ACS Appl. Mater. Interfaces*, 2022, **14**, 54127–54140.

106 J. Liao, Z. Ma, S. Liu, W. Li, X. Yang, M. E. Hilal, X. Zhou, Z. Yang and B. L. Khoo, *Adv. Funct. Mater.*, 2024, **34**, 2401930–2401942.

107 F. Oveissi, S. Naficy, T. Y. L. Le, D. F. Fletcher and F. Dehghani, *ACS Appl. Bio Mater.*, 2018, **1**, 2073–2081.

108 Q. Wang, X. Pan, J. Guo, L. Huang, L. Chen, X. Ma, S. Cao and Y. Ni, *Chem. Eng. J.*, 2021, **414**, 128903–128911.

109 S.-F. Sun, X.-Y. Zhao, C. Gao, L.-P. Xiao and R.-C. Sun, *Chem. Eng. J.*, 2024, **495**, 153781–153792.

110 X.-F. Sun, Y. Hao, Y. Cao and Q. Zeng, *Int. J. Biol. Macromol.*, 2019, **127**, 511–519.

111 J. Shen, M. Cai, G. Li, C. F. Guo, X. Qiu and Y. Qian, *Adv. Funct. Mater.*, 2024, **35**, 2413597–2413607.

112 X. Pan, J. Pan, X. Li, Z. Wang, Y. Ni and Q. Wang, *Adv. Mater.*, 2024, e2406671, DOI: [10.1002/adma.202406671](https://doi.org/10.1002/adma.202406671).

113 T. U. Nguyen, K. E. Watkins and V. Kishore, *J. Biomed. Mater. Res., Part A*, 2019, **107**, 1541–1550.

114 J. Kim, G. Zhang, M. Shi and Z. Suo, *Science*, 2021, **374**, 212–216.

115 Y. Miao, Z. Tang, Q. Zhang, A. Reheman, H. Xiao, M. Zhang, K. Liu, L. Huang, L. Chen and H. Wu, *ACS Appl. Polym. Mater.*, 2022, **4**, 1448–1456.

116 M. M  ller, B. Urban, B. Reis, X. Yu, A. L. Grab, E. A. Cavalcanti-Adam and D. Kuckling, *Polymers*, 2018, **10**, 1314–1332.

117 H. Xiu, H. Zhao, L. Dai, J. Li, Z. Wang, Y. Cui, Y. Bai, X. Zheng and J. Li, *Int. J. Biol. Macromol.*, 2022, **213**, 226–233.

118 Z. F. Zeng, Y. Q. Yang, X. W. Pang, B. Jiang, L. X. Gong, Z. Liu, L. Peng and S. N. Li, *Adv. Funct. Mater.*, 2024, **34**, 2409855–2409864.

119 P. Schlee, O. Hosseinaei, D. Baker, A. Landm  r, P. Tomani, M. J. Mostazo-L  pez, D. Cazorla-Amor  s, S. Herou and M.-M. Titirici, *Carbon*, 2019, **145**, 470–480.

120 L. Wu, S. Huang, J. Zheng, Z. Qiu, X. Lin and Y. Qin, *Int. J. Biol. Macromol.*, 2019, **140**, 538–545.

121 J. Zhu, Y. Luo, J. Wang, J. Yu, Q. Liu, J. Liu, R. Chen, P. Liu and J. Wang, *J. Mol. Liq.*, 2022, **368**, 120744–120752.

122 J. Hou, D. Lv, Y. Sun, P. Wang, Q. Zhang and J. Sundell, *Int. J. Environ. Res. Public Health*, 2020, **17**, 4069–4081.

123 Y. Ren, Y. Yang, J. Zhang, S. Ge, H. Ye, Y. Shi, C. Xia, Y. Sheng and Z. Zhang, *ACS Appl. Mater. Interfaces*, 2022, **14**, 47176–47187.

124 M. Siahkamari, S. Emmanuel, D. B. Hodge and M. Nejad, *ACS Sustainable Chem. Eng.*, 2022, **10**, 3430–3441.

125 S. Gonz  lez-Rodr  guez, T. A. Lu-Chau, X. Chen, G. Eibes, A. Pizzi, G. Feijoo and M. T. Moreira, *Ind. Crops Prod.*, 2022, **186**, 115253–115263.

126 K. A. Henn, S. Forssell, A. Pietil  inen, N. Forsman, I. Smal, P. Nousiainen, R. P. Bangalore Ashok, P. Oinas and M.   sterberg, *Green Chem.*, 2022, **24**, 6487–6500.

127 C. Huang, Z. Peng, J. Li, X. Li, X. Jiang and Y. Dong, *Ind. Crops Prod.*, 2022, **187**, 115388–115499.

128 J. Zheng, W. Zhao, L. Song, H. Wang, H. Yan, G. Chen, C. Han and J. Zhang, *Green Energy Environ.*, 2023, **8**, 626–653.

129 A. Arias, S. Gonz  lez-Garc  a, S. Gonz  lez-Rodr  guez, G. Feijoo and M. T. Moreira, *Sci. Total Environ.*, 2020, **738**, 140357–140370.

130 L. Wang, L. Lagerquist, Y. Zhang, R. Koppolu, T. Tirri, I. Sulaeva, S. V. Schoultz, L. V  h  salo, A. Pranovich, T. Rosenau, P. C. Eklund, S. Willf  r, C. Xu and X. Wang, *ACS Sustainable Chem. Eng.*, 2020, **8**, 13517–13526.

131 Y. Zhang, N. Li, Z. Chen, C. Ding, Q. Zheng, J. Xu and Q. Meng, *Polymers*, 2020, **12**, 2805–2818.

132 X. Shi, S. Gao, C. Jin, D. Zhang, C. Lai, C. Wang, F. Chu, A. J. Ragauskas and M. Li, *Green Chem.*, 2023, **25**, 5907–5915.

133 G. Yang, Z. Gong, X. Luo, L. Chen and L. Shuai, *Nature*, 2023, **621**, 511–515.

134 G. Yang, Z. Gong, B. Zhou, X. Luo, J. Liu, G. Du, C. Zhao and L. Shuai, *Green Chem.*, 2024, **26**, 753–759.

135 S. Pradyawong, G. Qi, N. Li, X. S. Sun and D. Wang, *Int. J. Adhes. Adhes.*, 2017, **75**, 66–73.

136 Y. Zhu, R. Bian, Y. Yu, J. Li, C. Li, Y. Lyu, X. Li, J. Luo and J. Li, *Chem. Eng. J.*, 2024, **494**, 152914–152927.

137 A. F. Ang, Z. Ashaari, S. H. Lee, P. Md Tahir and R. Halis, *Int. J. Adhes. Adhes.*, 2019, **95**, 102408–102419.

138 L. Dessbesell, M. Paleologou, M. Leitch, R. Pulkki and C. Xu, *Renewable Sustainable Energy Rev.*, 2020, **123**, 109768–109778.

139 B. Zhan, L. Zhang, Y. Deng and L. Yan, *Green Chem.*, 2023, **25**, 10061–10071.

140 Y. Zhou, J. Luo, Q. Jing, S. Ge, S. Chen, Z. Guo, J. Li, Z. Liu, P. He, X. He and B. B. Xu, *Adv. Funct. Mater.*, 2024, **34**, 2406557–2406566.

141 Z. Liu, T. Liu, Y. Li, X. Zhang, Y. Xu, J. Li and Q. Gao, *J. Cleaner Prod.*, 2022, **366**, 132906–132914.

142 S. Ebnesajjad, in *Handbook of Adhesives and Surface Preparation*, 2011, pp. 247–258, DOI: [10.1016/b978-1-4377-4461-3.10011-2](https://doi.org/10.1016/b978-1-4377-4461-3.10011-2).

143 W. Yang, M. Rallini, M. Natali, J. Kenny, P. Ma, W. Dong, L. Torre and D. Puglia, *Mater. Des.*, 2019, **161**, 55–63.

144 Y. Chen, J. Shen, W. Wang, L. Lin, R. Lv, S. Zhang and J. Ma, *Int. J. Biol. Macromol.*, 2023, **242**, 124462–124470.